Interlinking positive and negative feedback loops creates a tunable motif in gene regulatory networks

Xiao-Jun Tian, Xiao-Peng Zhang, Feng Liu,* and Wei Wang†
Department of Physics and National Laboratory of Solid State Microstructures, Nanjing University, Nanjing 210093, China
(Received 15 January 2009; revised manuscript received 11 June 2009; published 31 July 2009)

Positive and negative feedback loops are often coupled to perform various functions in gene regulatory networks, acting as bistable switches, oscillators, and excitable devices. It is implied that such a system with interlinked positive and negative feedback loops is a flexible motif that can modulate itself among various functions. Here, we developed a minimal model for the system and systematically explored its dynamics and performance advantage in response to stimuli in a unifying framework. The system indeed displays diverse behaviors when the strength of feedback loops is changed. First, the system can be tunable from monostability to bistability by increasing the strength of positive feedback, and the bistability regime is modulated by the strength of negative feedback. Second, the system undergoes transitions from bistability to excitability and to oscillation with increasing the strength of negative feedback, and the reverse conversion occurs by enhancing the strength of positive feedback. Third, the system is more flexible than a single feedback loop; it can produce robust larger-amplitude oscillations over a wider stimulus regime compared with a single time-delayed negative feedback loop. Furthermore, the tunability of the system depends mainly on the topology of coupled feedback loops but less on the exact parameter values or the mode of interactions between model components. Thus, our results interpret why such a system represents a tunable motif and can accomplish various functions. These also suggest that coupled feedback loops can act as toolboxes for engineering diverse functional circuits in synthetic biology.

DOI: 10.1103/PhysRevE.80.011926 PACS number(s): 87.16.Yc, 05.45.−a, 87.17.Aa

I. INTRODUCTION

Feedback is one of the most ubiquitous control modes in cellular signaling networks. It can be defined as the property of a system to use its output as (a part of) its input to adjust itself [1]. Positive feedback loops (PFLs) and negative feedback loops (NFLs) have been identified in various gene regulatory networks. It has been demonstrated that NFLs can act as noise suppressors [2], oscillators [3], and linearizers [4], and that PFLs can behave as switches and memory modules [5,6].

Interestingly, positive and negative feedback loops are often interlinked to play a variety of roles (Fig. 1) although a single positive or negative feedback loop can also perform these functions under certain conditions. For example, although a single positive feedback loop with ultrasensitivity is able to act as a bistable switch, additional negative feedback loops are involved in bistable systems such as the yeast galactose-utilization network [7,8] [Fig. 1(a)], the long-term memory system [9,10] [Fig. 1(b)], and the mitogen-activated protein kinase (MAPK) 1,2/protein kinase C (PKC) signaling network [11,12] [Fig. 1(c)]. Similarly, although a single negative feedback loop with a long-time delay can produce sustained oscillations, many oscillators also recruit additional positive feedback loops, as observed in circadian clocks [13,14] [Fig. 1(d)], eukaryotic cell cycle [15,16] [Fig. 1(e)], the p53-Mdm2 oscillator in response to DNA damage [17] [Fig. 1(f)], and the Ca^{2+} spikes/oscillations [18] [Fig. 1(g)]. Moreover, excitability can occur in systems with combined positive and negative feedback loops, as exemplified by a transient differentiation into competence in *bacillus subtilis* [19–21] [Fig. 1(h)]. Thus, an issue naturally arises concerning why and how positive and negative feedback loops interact to perform diverse functions.

On the other hand, it has been shown that linking fast and slow positive feedback loops creates an optimal switch in cell signaling [22,23]. It has also been demonstrated that combined positive and negative feedback loops are superior to single feedback loops as switches [24,25] or as oscillators

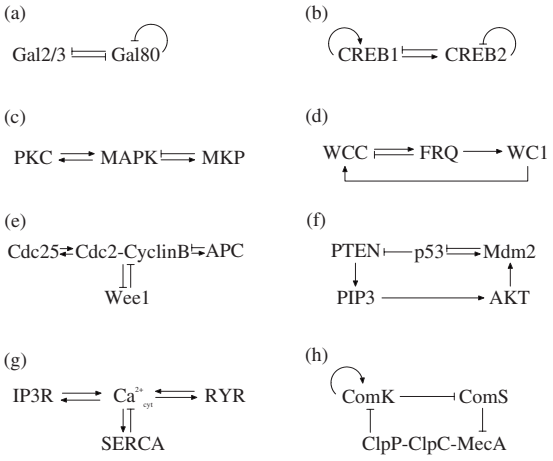

FIG. 1. Examples of biological systems with interlinked positive and negative feedback loops. (a) The yeast galactose-utilization network, (b) formation of long-term memory, (c) the MAPK/PKC system, (d) the *Neurospora crassa* circadian clock, (e) the mitotic trigger in Xenopus, (f) the p53-Mdm2 oscillator in response to DNA damage, (g) Ca^{2+} spikes/oscillations, and (h) the transient cellular differentiation in *bacillus subtilis*.

*fliu@nju.edu.cn
†wangwei@nju.edu.cn

 ©2009 The American Physical Society

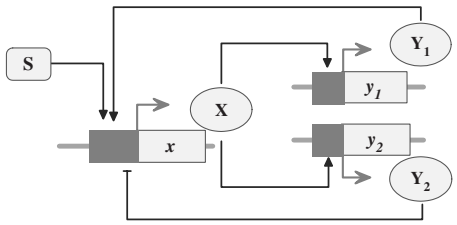

FIG. 2. Schematic depiction of the model. The transcription factor X induces expression of genes y_1 and y_2. The activation of X by Y_1 encloses a positive feedback while the repression of X by Y_2 yields a negative feedback. Thus, the circuit is composed of interlinked positive and negative feedback loops. S is an external stimulus assumed to promote the expression of x independently of Y_1 and Y_2.

[26]. However, these studies focused on a performance advantage of coupled feedback loops in terms of certain dynamic characteristic. It would be intriguing to systematically investigate the underlying design principle of the system with coupled positive and negative feedback loops, and to reveal its functions in a unifying framework.

Motivated by the above considerations, we construct a minimal model by keeping the essential feature of all the systems shown in Fig. 1, i.e., interlinked positive and negative feedback loops. A similar approach has been adopted in Refs. [22,24,25]. We explore the dynamics of the model system via numerical simulations and bifurcation analysis. We find that the system can tune itself to exhibit diverse behaviors such as monostability, bistability, excitability, and oscillation by changing the feedback strength. First, the system undergoes a transition from monostability to reversible and irreversible bistability with increasing the strength of positive feedback. Second, the system is tunable from irreversible bistability to excitability and to oscillation with enhancing the strength of negative feedback, and the reverse conversion occurs with increasing the strength of positive feedback. Third, compared with a single time-delayed negative feedback loop, coupled feedback loops can generate larger-amplitude oscillations over a wider stimulus regime. Fourth, an overall picture of the tunability of the system is presented in a two-parameter bifurcation diagram. Such tunability holds true for a wide variety of parameter values. We also associate the dynamic behaviors of the system with specific physiological processes in cellular systems. The paper is organized as follows. A model of coupled positive and negative feedback loops is presented in Sec. II. We describe various behaviors of the system and the underlying mechanisms in Sec. III. Discussion and conclusion is presented in Sec. IV.

II. MODEL

Based on the regulatory networks shown in Fig. 1, an abstract model is developed by keeping the essential feature of all the systems, namely, coupled positive and negative feedback loops. The model is constructed as follows (Fig. 2). X is the core component of the model system as a transcription factor, inducing expression of genes y_1 and y_2 to produce its own activator Y_1 and repressor Y_2. Thus, the activation of X by Y_1 encloses a positive feedback, whereas the repression of X by Y_2 yields a negative feedback. S is an external stimulus, which is assumed to promote the expression of gene x independently of Y_1 and Y_2. The level of protein X is regarded as the output of the system.

The dynamics of the system are described by the following ordinary differential equations (ODEs):

$$\frac{d[X]}{dt} = V_x \frac{\left(\frac{[Y_1]}{K_{y_1x}}\right)^n}{1+\left(\frac{[Y_1]}{K_{y_1x}}\right)^n+\left(\frac{[Y_2]}{K_{y_2x}}\right)^n} - d_x[X] + b_xS, \quad (1)$$

$$\frac{d[Y_1]}{dt} = V_{y_1} \frac{\left(\frac{[X]}{K_{xy_1}}\right)^n}{1+\left(\frac{[X]}{K_{xy_1}}\right)^n} - d_{y_1}[Y_1] + b_{y_1}, \quad (2)$$

$$\frac{d[Y_2]}{dt} = V_{y_2} \frac{\left(\frac{[X]}{K_{xy_2}}\right)^n}{1+\left(\frac{[X]}{K_{xy_2}}\right)^n} - d_{y_2}[Y_2] + b_{y_2}. \quad (3)$$

$[X]$, $[Y_1]$, and $[Y_2]$ denote the concentrations of X, Y_1, and Y_2, respectively. The regulated expression of genes is represented by Hill functions with cooperativity exponent n. Y_1 and Y_2 compete to control the transcription of x. Each species is assumed to degrade at a rate, which is proportional to its concentration. Suppose that the basal synthesis rate of X is proportional to the upstream stimulus $S(S \geq 0)$ while that of Y_1 and Y_2 is constant.

V_{y_1} and V_{y_2} can be taken as the strength of positive and negative feedback, respectively. The system is converted into a single positive feedback loop when setting $V_{y_2}=0$ or a single negative feedback loop when setting $V_{y_1}=0$. Since we aim to explore how the balance between the PFL and the NFL tunes the function of the system, we change only the values of V_{y_1} and V_{y_2} while keeping the other parameters fixed unless specified otherwise. All the parameters are dimensionless and their values are taken as follows: $V_x=1$, $K_{xy_1}=1$, $K_{xy_2}=1$, $K_{y_1x}=1$, $K_{y_2x}=1$, $b_x=0.01$, $b_{y_1}=0.1$, $b_{y_2}=0.1$, $d_x=0.2$, $d_{y_1}=0.2$, $d_{y_2}=0.02$, and $n=2$. It is noted that all the above values are arbitrarily chosen so that the system may be more tunable in a larger parameter space spanned by V_{y_1} and V_{y_2}.

To investigate whether the main conclusion drawn also holds true when X is regulated by Y_1 and Y_2 in a noncompetitive way, a simple variant of the above model is considered and described as follows:

$$\frac{d[X]}{dt} = V_x \frac{\left(\frac{[Y_1]}{K_{y_1x}}\right)^n}{\left\{1+\left(\frac{[Y_1]}{K_{y_1x}}\right)^n\right\}\left\{1+\left(\frac{[Y_2]}{K_{y_2x}}\right)^n\right\}} - d_x[X] + b_xS, \quad (4)$$

$$\frac{d[Y_1]}{dt} = V_{y_1}\frac{\left(\frac{[X]}{K_{xy_1}}\right)^n}{1+\left(\frac{[X]}{K_{xy_1}}\right)^n} - d_{y_1}[Y_1] + b_{y_1}, \tag{5}$$

$$\frac{d[Y_2]}{dt} = V_{y_2}\frac{\left(\frac{[X]}{K_{xy_2}}\right)^n}{1+\left(\frac{[X]}{K_{xy_2}}\right)^n} - d_{y_2}[Y_2] + b_{y_2}. \tag{6}$$

Parameters in Eqs. (4)–(6) have the same meanings and values as in Eqs. (1)–(3) except for $b_{y_1}=0.02$ and $b_{y_2}=0.05$ [see Fig. 11(f)].

Time delay is ubiquitous in gene regulatory systems, including the time needed to perform transcription and translation and to transport chemical species between cellular compartments [27]. To explore the effect of time delay on the competitive model, we also perform simulations with explicit time delay (see Figs. 6–8). The expression rate of each gene at time t depends on the concentrations of proteins at time $t-\tau$, where τ is the time delay required for the transcription and translation. The model with time delay is described by the following delay differential equations (DDEs):

$$\frac{d[X]}{dt} = V_x\frac{\left(\frac{[Y_1]_{t-\tau}}{K_{y_1x}}\right)^n}{1+\left(\frac{[Y_1]_{t-\tau}}{K_{y_1x}}\right)^n+\left(\frac{[Y_2]_{t-\tau}}{K_{y_2x}}\right)^n} - d_x[X] + b_xS, \tag{7}$$

$$\frac{d[Y_1]}{dt} = V_{y_1}\frac{\left(\frac{[X]_{t-\tau}}{K_{xy_1}}\right)^n}{1+\left(\frac{[X]_{t-\tau}}{K_{xy_1}}\right)^n} - d_{y_1}[Y_1] + b_{y_1}, \tag{8}$$

$$\frac{d[Y_2]}{dt} = V_{y_2}\frac{\left(\frac{[X]_{t-\tau}}{K_{xy_2}}\right)^n}{1+\left(\frac{[X]_{t-\tau}}{K_{xy_2}}\right)^n} - d_{y_2}[Y_2] + b_{y_2}. \tag{9}$$

Parameters in Eqs. (7)–(9) have the same denotation and values as in Eqs. (1)–(3) except for $V_x=20$. For simplicity, the same time delay is assumed for the expression of three genes.

To numerically solve the above equations, ODEs and DDEs were separately integrated using ODE23 and DDE23 in MATLAB or XPP. Numerical bifurcation analysis of the ODEs was performed with OSCILL8 [28].

III. RESULTS

As we shall see, the model system can exhibit diverse behaviors such as monostability, bistability, excitability, and oscillation when the values of V_{y_1} and V_{y_2} are varied. That is, the system is tunable by balancing the strength of positive and negative feedback. Here, we report the typical behaviors of the system and also relate them to specific physiological processes in cellular signaling systems.

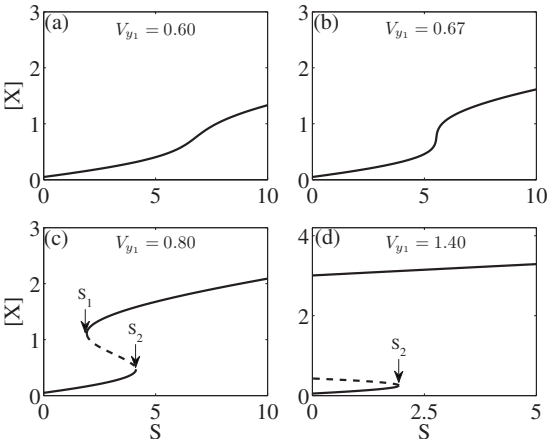

FIG. 3. The signal-response curves of the system. When the strength of positive feedback is increased from (a) 0.6, (b) 0.67 to (c) 0.80 and (d) 1.4, the system undergoes the transition from monostability to bistability. The strength of negative feedback is fixed at $V_{y_2}=0.01$. Solid and dashed lines separately denote stable and unstable states. S_1 and S_2 represent the saddle-node bifurcation points.

A. Adding a negative feedback loop makes a bistable switch more flexible

Positive feedback is known to be an essential ingredient for bistability in biochemical systems [5]. Here, we show that the system can exhibit monostability and bistability with increasing V_{y_1} while V_{y_2} is kept fixed at 0.01. In response to a constant stimulus, the system converges to a steady state after transients. The signal-response relationship is explored in terms of bifurcation diagram (Fig. 3).

With a small value of V_{y_1}, the system is monostable with a single steady state, which is globally stable [Fig. 3(a)]. Here, the steady-state value of $[X]$ rises monotonically with increasing signal intensity S. When V_{y_1} is further increased, the system exhibits ultrasensitivity but is still monostable [Fig. 3(b)]. For $V_{y_1}=0.8$, the system can exhibit bistability when S falls in the range between two saddle-node bifurcation points S_1 and S_2 [Fig. 3(c)]. Clearly, the system exhibits some hysteresis, i.e., $[X]$ converges to a low or high state depending on the initial condition. Therefore, the system has the potential to remember the stimulus long after it has been removed, acting as a memory module [6,7]. Moreover, continuous stimuli can be converted into discontinuous switch-like responses, which can be either reversible or irreversible, corresponding to a toggle switch [Fig. 3(c)] or a one-way switch [Fig. 3(d)], respectively. The one-way switch is an extreme manifestation of hysteresis, i.e., its top stable solution branches into the negative domain but is actually restricted within the positive domain to be physically meaningful. Based on such hysteresis and irreversibility, bistable

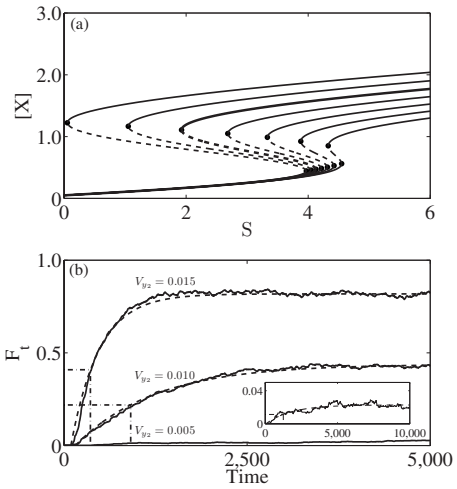

FIG. 4. The effect of negative feedback on the bistability and flexibility of a bistable switch. (a) The signal-response curves of the system. The strength of negative feedback is separately 0.0, 0.005, 0.01, 0.015, 0.02, 0.025, and 0.03 (from left to right), while the strength of positive feedback is fixed at 0.8. Accordingly, the bistability regime can be remarkably modulated. Note that the thick line is the same as that in Fig. 3(c). (b) The time courses of "fraction of transition" F_t for V_{y_2}=0.005, 0.01, or 0.015 (solid lines, from bottom to up). The dashed lines represent an exponential fitting. Initially, all cells are settled in the high state and driven by the same noisy stimulus $S(t)=S_0[1+\xi(t)]$, where $\xi(t)$ is a Gaussian white noise with mean 0 and variance 1, and S_0=3. The inset shows a long-time course of F_t for the case of V_{y_2}=0.005.

switches can make a reliable decision in many physiological processes, as in the yeast galactose-utilization network [7,8], the long-term memory systems [9,10], and the MAPK/PKC signaling network [11,12]. Interestingly, these bistable systems include both negative and positive feedback loops.

Given that a single PFL with ultrasensitivity is sufficient to create bistability, it is intriguing to address the role of an additional NFL in the above bistable systems. To this end, we change the strength of negative feedback to explore its effect on bistability while the strength of positive feedback is fixed at V_{y_1}=0.8. With increasing V_{y_2}, the bistability regime becomes narrow while the upper threshold changes moderately [Fig. 4(a)]. This is consistent with the results in Refs. [6,7]. It seems that strong negative feedback tends to deteriorate bistability. So why is this "undesirable" negative feedback loop involved? In fact, it makes the bistable switch adapt to fluctuating environments.

To see that clearly, we explore the dynamics of the system in response to a noisy stimulus. We assume that a population of 1000 cells is simultaneously driven by the same noisy stimulus $S(t)=S_0[1+\xi(t)]$, where $\xi(t)$ is a Gaussian white noise and S_0=3. Suppose that all cells are initially in the high state, then some cells may flip to the low state driven by the noise. We define the ratio of the number of cells in the low state to the number of all cells as the "fraction of transition" F_t at each moment. Moreover, the time taken for F_t to reach the midpoint between its initial and steady-state values is called the response time t_r.

The time courses of F_t for different V_{y_2} are shown in Fig. 4(b). With V_{y_2}=0.005, it takes a relatively long time (>5000) for F_t to reach a steady state (with t_r=1250), where only about 2% of the cells flip to the low state. That is, most of the cells are trapped in the high state for a long time. Thus, the system with a weaker NFL is almost unresponsive to the fluctuating environment. As V_{y_2} rises, the system becomes more sensitive to the stimulus, and it takes less time for F_t to reach a steady state (with t_r=910 and 360 for V_{y_2}=0.01 and 0.015, respectively), where its value is significantly larger than 0. With V_{y_2}=0.015, for example, about 80% of the cells are driven to the low state. Thus, adding a stronger NFL can make the bistable system more flexible and adaptable to fluctuating environments through stochastic switching, avoiding an improper trapping in either of two states [29]. It has been reported that stochastic switching between alternative states can act as a survival strategy in fluctuating environments [30]. Therefore, while a positive feedback loop is crucial for the bistability, adding a negative feedback loop can make the system more flexible and improve its adaptability in fluctuating environments.

B. Enhancing the negative feedback can tune the system from bistability to oscillation

In contrast to positive feedback, negative feedback has the potential to evoke oscillations in the system. We begin with the one-way switch in Fig. 3(d) and then increase the strength of negative feedback to explore its influence on the output of the system. The strength of positive feedback is fixed at V_{y_1}=1.4. We find that the system undergoes transitions from bistability to excitability and to oscillation with increasing V_{y_2} (see Fig. 5).

The system first acts as a one-way switch [Fig. 5(a)]. When driven by a pulse input, [X] settles in a high-level state [Fig. 5(b)]; that is, the system exhibits irreversibility. With a moderate increase in V_{y_2}, the system exhibits excitability when the signal intensity falls in the range between S_1 and H_1 [Fig. 5(c)]. In this case, there are three steady states, and only the lower one is stable while the upper and middle ones are unstable. In contrast to a bistable system, the excitable system completely recovers to the initial state without any irreversibility after the pulse signal. As seen in Fig. 5(d), a relatively small pulse input drives [X] into the upper state. Owing to its instability, [X] returns to the original lower state after short excursion, thus creating a transient large-amplitude pulse. That is, the excitable system can generate a transient pulse rather than an irreversible flip. In fact, many transient cellular processes originate from this excitability. For example, the transient differentiation into competence in *bacillus subtilis* results from such excitability, and the core regulatory network involved is also composed of coupled positive and negative feedback loops [19–21].

When V_{y_2} is further increased, the system displays limit-cycle oscillations when the stimulus amplitude falls in the range between two Hopf bifurcation points H_1 and H_2 [Fig. 5(e)]. Since no explicit time delay exists in the negative feedback, the oscillations are based on the hysteresis created by the positive feedback [27,31]. That is, increasing the strength of negative feedback turns the hysteretic bistability [Fig. 5(a)] into stable oscillation [Fig. 5(e)]. Here, the nega-

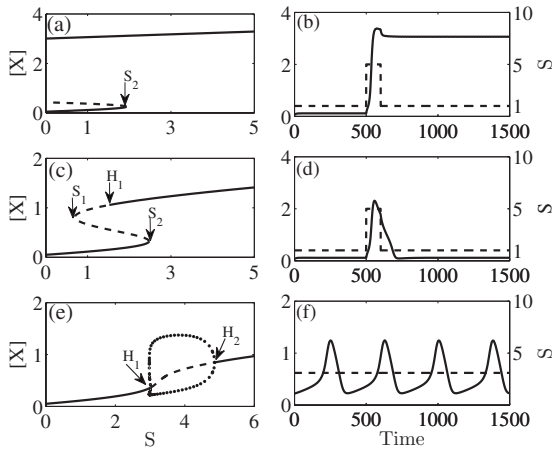

FIG. 5. The dynamics of the system. While the strength of positive feedback is fixed at 1.4, the strength of negative feedback is increased from 0.01 to 0.13 and 0.2 (from top to bottom). The left columns show the signal-response curves (with the same convention as in Fig. 3); the right columns display the corresponding time course of $[X]$ in response to [(b) and (d)] a pulse input or (f) a constant stimulus with $S=3.1$, with the dashed lines representing the input signal. In panel (e), H_1 and H_2 denote Hopf bifurcation points, and the solid/open circles surrounding the unstable state separately represent the maxima and minima of $[X]$ during a stable/unstable oscillation. Clearly, the system undergoes the transitions from bistability to excitability and to relaxation oscillation with increasing V_{y_2}. Note that Fig. 5(a) is the same as Fig. 3(d) and is shown for facilitating comparison.

tive feedback is strong enough to drive $[X]$ back and forth between the two discrete states created by the PFL. Such a hysteresis-driven oscillation is a kind of relaxation oscillation; $[X]$ first rises gradually and then drops rapidly over one cycle [Fig. 5(f)]. Many physiological rhythmicity can be explained in terms of such relaxation oscillation. The eukaryotic cell cycle, as a prominent example of robust oscillations, is regulated by coupled positive and negative feedback loops. It was first predicted theoretically [32] and then demonstrated experimentally in *Xenopus laevis* egg extracts [15,33] that the cell cycle transition is driven by hysteresis. Another remarkable oscillator regulated by interlinked positive and negative feedback loops is the circadian clock as observed in *Neurospora crassa* [13], *Drosophila*, and mouse [14].

It has been illustrated above that, without time delay, the coupled positive and negative loops can generate sustained oscillations. But time delay is ubiquitous in gene regulatory systems. It was shown that a single NFL with a long-time delay is sufficient to generate oscillations [3]. Then, what is the role of an additional PFL in the above systems? We find that the PFL is necessary for sustained oscillations when the time delay involved in the NFL is not large enough (the strength of negative feedback is fixed at $V_{y_2}=2$ in Figs. 6–8). As shown in Fig. 6(a), without PFL ($V_{y_1}=0$), the NFL itself can generate oscillations only with a large time delay ($\tau>40$ in this case). With $\tau=50$, for example, $[X]$ can oscillate persistently during the period between 0 and 2000, but the oscillation is arrested immediately at $t=2000$ when the time delay is reduced abruptly to $\tau=5$. However, the

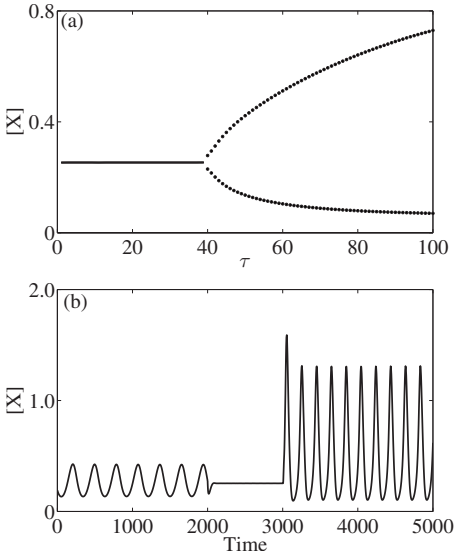

FIG. 6. The effect of positive feedback on the generation of oscillations in the presence of time delay in feedback loops. The strength of negative feedback is $V_{y_2}=2$. (a) The bifurcation diagram of the delayed model without positive feedback ($V_{y_1}=0$). (b) The time course of $[X]$ in response to a constant stimulus with $S=1$ (see text for details). Clearly, the positive feedback is necessary for oscillations when the time delay is not long enough.

oscillation is resumed by involving the PFL with $V_{y_1}=1$ at $t=3000$ [Fig. 6(b)]. Thus, the PFL is essential for oscillations when the NFL has a small time delay.

Moreover, compared with a single NFL, coupled feedback loops generate larger-amplitude oscillations over a wider stimulus regime [separately comparing Fig. 7(a) with Fig. 7(c) and Fig. 7(b) with Fig. 7(d)]. That is, the coupled feedback loops can produce more robust oscillations than single delayed NFLs. Furthermore, in response to the same noisy stimulus, the fluctuations of the oscillations generated in the coupled feedback loops are smaller than those in the single delayed NFL, while the corresponding phase portraits in the

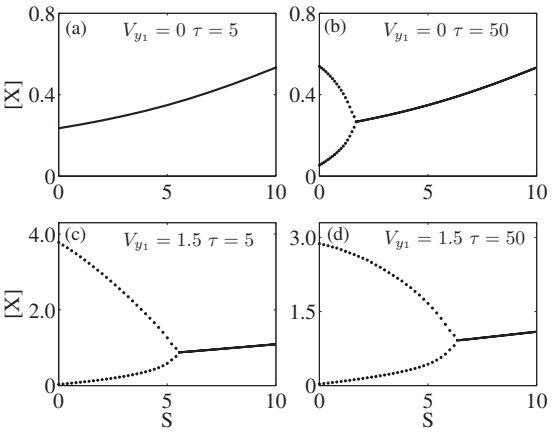

FIG. 7. The signal-response curves of the system with time delay. The strength of negative feedback is $V_{y_2}=2$. (a) $V_{y_1}=0$ and $\tau=5$; (b) $V_{y_1}=0$ and $\tau=50$; (c) $V_{y_1}=1.5$ and $\tau=5$; (d) $V_{y_1}=1.5$ and $\tau=50$. The coupled positive and negative feedback loops can generate larger-amplitude oscillations over a wider stimulus regime.

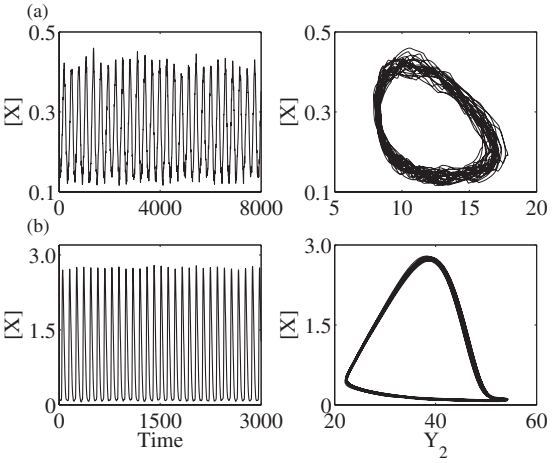

FIG. 8. The dynamics of the system in response to a noisy stimulus. The left columns show the time course of $[X]$, while the right ones show the corresponding phase plots of $[X]$ vs Y_2. The strength of positive feedback is $V_{y_1}=0$ (a) or $V_{y_1}=1.5$ (b), while the strength of negative feedback is $V_{y_2}=2$ and the time delay is $\tau=50$ for both cases. The noisy stimulus is a series of uniformly distributed pseudorandom numbers between 0.5 and 1.5.

coupled feedback loops are more closer to the limit cycle produced in response to a deterministic signal [Figs. 8(a) and 8(b)]. Therefore, the positive feedback not only helps the NFL with a short-time delay to oscillate but also contributes to the robustness of oscillations.

C. Enhancing the positive feedback can reverse the system dynamics from oscillation to bistability

It has been demonstrated above that the negative feedback can tune dynamic properties of the system. Now we turn to explore whether the positive feedback can exert a similar influence on the tunability of the system. We begin with the relaxation oscillation in Figs. 9(a) and 9(b), and then increase the strength of positive feedback. Here, the strength of negative feedback is fixed at $V_{y_2}=0.2$. The system exhibits excitability when V_{y_1} is increased from 1.4 to 1.8 [Figs. 9(c) and 9(d)]. For $V_{y_1}=2.2$, the system returns to be a one-way switch [Figs. 9(e) and 9(f)]. Therefore, a conversion from oscillation to bistability occurs when the strength of positive feedback is enhanced. In fact, such a conversion has been implied in Fig. 5 by reducing the strength of negative feedback. In this sense, two ways can be used to convert oscillation to bistability: enhancing the positive feedback or reducing the negative feedback. Similarly, the conversion from bistability to oscillation can be realized by enhancing the negative feedback or weakening the positive feedback. Moreover, a match between the strength of two feedback loops is necessary for desirable behaviors. Thus, it is intriguing to investigate the dynamics of the system when simultaneously changing the strength of negative and positive feedback.

D. Fine tuning the system by simultaneously altering the strength of two feedback loops

Simultaneously tuning the strength of positive and negative feedbacks, V_{y_1} and V_{y_2}, is a general way to produce

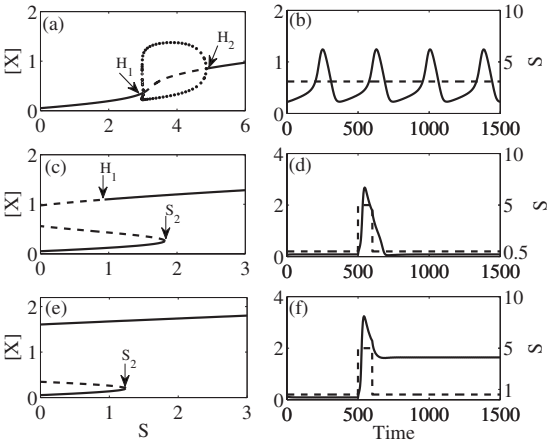

FIG. 9. The dynamics of the system. While the strength of negative feedback is fixed at 0.2, the strength of positive feedback is increased from 1.4 to 1.8 and 2.2 (from top to bottom). The left columns show the signal-response curves; the right columns display the corresponding time course of $[X]$ in response to a constant stimulus with (b) $S=3.1$ or [(d) and (f)] a pulse input, with the dashed lines representing the input signal. The same convention as in Fig. 5. Clearly, the system undergoes the transitions from relaxation oscillation to excitability and to bistability. Note that Figs. 9(a) and 9(b) are the same as Figs. 5(e) and 5(f), respectively, and are shown for facilitating comparison.

desirable behaviors. A two-parameter bifurcation diagram, which heavily depends on the stimulus intensity S, is shown in Fig. 10 to give an overview of the tunability of the system with $S=1$. Clearly, the dynamics of the system are mainly classified into four regimes: monostability, bistability, excitability, and oscillation, which are separated by saddle-node and Hopf bifurcation points, respectively. Consequently, we can obtain desired behaviors by setting the values of V_{y_1} and V_{y_2} in the corresponding regions. For $S=1$, for example, the system exhibits bistability with $V_{y_1}=2$ and $V_{y_2}=0.1$, monostability with $V_{y_1}=1$ and $V_{y_2}=0.5$, excitability with $V_{y_1}=2.5$ and $V_{y_2}=0.4$, and oscillation with $V_{y_1}=4$ and $V_{y_2}=1$. Therefore, cooperatively tuning the strength of two feedback loops is the general way to realize various behaviors and functions.

To validate the generality of the above conclusion, we also change the values of the parameters except V_{y_1} and V_{y_2},

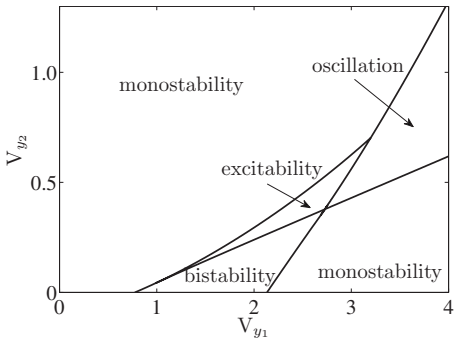

FIG. 10. Two-parameter bifurcation diagram in the space spanned by V_{y_1} and V_{y_2} with $S=1$. The dynamics of the system are mainly classified into four regimes: monostability, bistability, excitability, and oscillation.

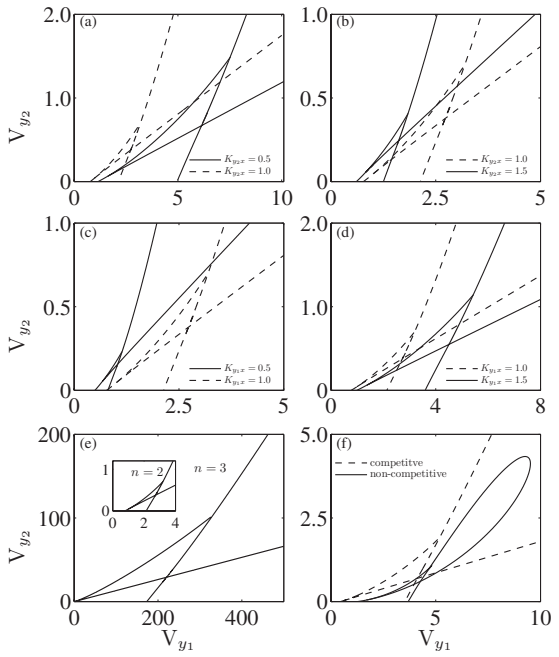

FIG. 11. Dependence of the tunability of the system on parameter values and the mode of interactions between model components. Two-parameter bifurcation diagrams for different values of [(a) and (b)] K_{y_2x}, [(c) and (d)] K_{y_1x}, (e) n, and (f) for the competitive and the noncompetitive model. The parameter values and the interaction modes are marked in the panels. The constant stimulus is always set to $S=1$.

and analyze their effects on the two-parameter bifurcation diagram. Generally, the four dynamic regimes still exist while the sizes and locations of the corresponding regimes vary with parameter values. On the one hand, the increase (or decrease) of V_x, b_x, b_{y_1}, K_{xy_2}, K_{y_2x}, or d_{y_2} moves the boundaries of the four dynamic regimes to smaller (or larger) values of V_{y_1} and V_{y_2}, as exemplified by the case of K_{y_2x} [Figs. 11(a) and 11(b)]. This shift occurs because the increase in these parameter values indirectly enhances the activation intensity of Y_1 and Y_2 by X. Thus, smaller values of V_{y_1} and V_{y_2} are needed to compensate. For example, the increase in K_{y_2x} weakens the repression effect of X by Y_2, thereby improving the production of X and then that of Y_1 and Y_2. As a result, smaller values of V_{y_1} and V_{y_2} are required to compensate.

On the other hand, the change in K_{xy_1}, K_{y_1x}, b_{y_2}, d_x, and d_{y_1} leads to the opposite effects. The increase (or decrease) of them shifts the boundaries to larger (smaller) values of V_{y_1} and V_{y_2}, as represented by the case of K_{y_1x} [Figs. 11(c) and 11(d)]. The increase in these parameter values indirectly reduces the activation intensity of Y_1 and Y_2 by X, and thus larger values of V_{y_1} and V_{y_2} are needed to compensate. For example, the increase in K_{y_1x} weakens the activation effect of X by Y_1, thereby decreasing the production of X and then that of Y_1 and Y_2. Consequently, larger values of V_{y_1} and V_{y_2} are required to compensate. Note that such a parameter compensation effect on the two-parameter diagram is consistent with Ref. [10].

Finally, the system is rather sensitive to the variation in the Hill coefficient n. As shown in Fig. 11(e), when n is changed form $n=2$ to $n=3$, the boundaries are shifted to larger values of V_{y_1} and V_{y_2} by two orders of magnitude. In fact, the Hill function with $n>1$ represents the source of ultrasensitivity, which is a prerequisite for bistability. Taken together, the conclusion drawn above generally holds true for a wide range of parameter values.

We also explore how the tunability of the coupled positive and negative feedback loops depends on the way Y_1 and Y_2 regulate X. Here, we consider a simple case where Y_1 and Y_2 regulate X in a noncompetitive manner [see Eqs. (4)–(6) in Sec. II]. As shown in Fig. 11(f), the four dynamic regimes still exist while the sizes and locations of the regimes change. Clearly, for the noncompetitive case, there exist smaller regimes for bistability, excitability, and oscillation. This shrink occurs because the noncompetitive interaction between components yields stronger repression of X by Y_2, suppressing the bistability or oscillation. Nevertheless, the tunability of the system is conserved. Therefore, the tunability is an intrinsic property of the system with coupled positive and negative feedback loops.

IV. DISCUSSION

We have demonstrated that the system with interlinked positive and negative feedback loops acts as a tunable motif, which manifests diverse behaviors when the feedback strength is varied. First, the system undergoes the transition from monostability to reversible and irreversible bistability with increasing the strength of positive feedback, and the bistability regime can be modulated by the strength of negative feedback. Second, the system can be fine tuned among bistability, excitability, and oscillation by changing the feedback strength. In summary, the system with coupled positive and negative feedback loops is a tunable motif such that the desirable dynamic behavior can be realized by tuning the feedback strength.

Our results interpret why positive and negative feedback loops are often interlinked in gene regulatory networks. Such systems can have performance advantages in terms of tunability, adaptability, and robustness. First, it is unnecessary to change the topology of such systems in order to perform distinct functions. It has recently been suggested that oscillators with both positive and negative feedback appear to evolve more easily [15,16,26]. Indeed, our results provide a plausible mechanism for the evolution of relaxation oscillators. That is, a bistable switch without or with weak negative feedback can gradually evolve to a relaxation oscillator by enhancing the negative feedback. Second, such systems are more flexible or robust than single feedback loops. Our results indicate that coupled feedback loops can adapt to fluctuating environments when acting as a bistable switch or can produce robust oscillations.

To explore the effect of time delay in feedback loops (due to transcription and translation) on the system dynamics, we explicitly add the time delay to the model. When the delay in the negative feedback is small, the positive feedback is needed for the system to oscillate. The presence of positive

feedback increases the oscillation amplitude and widens the stimulus regime for oscillation, thus promoting the robustness of oscillations. This is consistent with the previous results in Ref. [26]: involving a long-time delay in the negative feedback loop can generate oscillations, but adding a positive feedback loop can make the system more robust.

We have also shown that the tunability is an intrinsic property of the system with coupled positive and negative feedback loops because this property is conserved when changing the parameter values or the way Y_1 and Y_2 regulate the production of X. These suggest that the tunability of the system depends more on the topology of the gene regulatory network—coupled positive and negative feedback loops.

There are two limitations in the present study. The model is not developed for a specific system but for a general system of coupled positive and negative feedback loops. Our work only numerically shows how the system is tunable via changing the strength of feedback loops. It would be intriguing to further provide analytical conditions satisfied by parameter values for diverse dynamic behaviors. Moreover, we discuss how the system is tunable among only four typical behaviors: monostability, bistability, excitability, and oscillation, which have been identified in gene regulatory systems, while ignoring other more complex dynamic behaviors such as birhythmicity and chaos.

Simple gene circuits such as toggle switches and oscillators have been constructed consisting of single feedback loops in *Escherichia coli* [34,35]. A robust oscillator has also been built composed of coupled positive and negative feedback loops [36]. However, a synthetic circuit capable of multiple functions is still absent. Using the method of synthetic biology, the feedback strength can be tuned by either altering recruitment affinity or varying promoter strength [37]. Thus, a gene circuit consisting of coupled negative and positive feedback loops can be engineered to perform diverse functions by just tuning their strength.

ACKNOWLEDGMENTS

This work was supported by the NSFC (Contract No. 10604028), the National Basic Research Program of China (Contract No. 2007CB814806), NCET Contract No. 08-0269, and the SRF for ROCS, SEM.

[1] A. Y. Mitrophanov and E. A. Groisman, BioEssays **30**, 542 (2008).
[2] A. Becskei and L. Serrano, Nature (London) **405**, 590 (2000).
[3] D. M. Wolf and A. P. Arkin, Curr. Opin. Microbiol. **6**, 125 (2003).
[4] D. Nevozhay *et al.*, Proc. Natl. Acad. Sci. U.S.A. **106**, 5123 (2009).
[5] W. Xiong and J. E. Ferrell, Jr., Nature (London) **426**, 460 (2003).
[6] Z. Cheng, F. Liu, X.-P. Zhang, and W. Wang, FEBS Lett. **582**, 3776 (2008).
[7] M. Acar, A. Becskei, and A. van Oudenaarden, Nature (London) **435**, 228 (2005).
[8] S. A. Ramsey *et al.*, Nat. Genet. **38**, 1082 (2006).
[9] H. A. Mohamed *et al.*, J. Biol. Chem. **280**, 27035 (2005).
[10] H. Song *et al.*, Biophys. J. **92**, 3407 (2007).
[11] U. S. Bhalla and R. Iyengar, Chaos **11**, 221 (2001).
[12] U. S. Bhalla, P. T. Ram, and R. Iyengar, Science **297**, 1018 (2002).
[13] K. Lee, J. J. Loros, and J. C. Dunlap, Science **289**, 107 (2000).
[14] L. P. Shearman *et al.*, Science **288**, 1013 (2000).
[15] J. R. Pomerening, S. Y. Kim, and J. E. Ferrell, Jr., Cell **122**, 565 (2005).
[16] J. R. Pomerening, E. D. Sontag, and J. E. Ferrell, Jr., Nat. Cell Biol. **5**, 346 (2003).
[17] K. B. Wee, U. Surana, and B. D. Aguda, PLoS ONE **4**, e4407 (2009).
[18] J. Keizer, Y. X. Li, S. Stojilkovic, and J. Rinzel, Mol. Biol. Cell **6**, 945 (1995).
[19] G. M. Süel, J. Garcia-Ojalvo, L. M. Liberman, and M. B. Elowitz, Nature (London) **440**, 545 (2006).
[20] G. M. Süel *et al.*, Science **315**, 1716 (2007).
[21] H. Maamar, A. Raj, and D. Dubnau, Science **317**, 526 (2007).
[22] O. Brandman, J. E. Ferrell, Jr., R. Li, and T. Meyer, Science **310**, 496 (2005).
[23] X.-P. Zhang, Z. Cheng, F. Liu, and W. Wang, Phys. Rev. E **76**, 031924 (2007).
[24] D. Kim, Y.-K. Kwon, and K.-H. Cho, BioEssays **29**, 85 (2007).
[25] J.-R. Kim, Y. Yoon, and K.-H. Cho, Biophys. J. **94**, 359 (2008).
[26] T. Y.-C. Tsai *et al.*, Science **321**, 126 (2008).
[27] B. Novak and J. J. Tyson, Nat. Rev. Mol. Cell Biol. **9**, 981 (2008).
[28] See http://oscill8.sourceforge.net/.
[29] M. Kaern, T. C. Elston, W. J. Blake, and J. J. Collins, Nat. Rev. Genet. **6**, 451 (2005).
[30] M. Acar, J. T. Mettetal, and A. van Oudenaarden, Nat. Genet. **40**, 471 (2008).
[31] J. J. Tyson, K. C. Chen, and B. Novak, Curr. Opin. Cell Biol. **15**, 221 (2003).
[32] B. Novak and J. J. Tyson, J. Cell Sci. **106**, 1153 (1993).
[33] W. Sha *et al.*, Proc. Natl. Acad. Sci. U.S.A. **100**, 975 (2003).
[34] T. S. Gardner, C. R. Cantor, and J. J. Collins, Nature (London) **403**, 339 (2000).
[35] M. B. Elowitz and S. Leibler, Nature (London) **403**, 335 (2000).
[36] J. Stricker *et al.*, Nature (London) **456**, 516 (2008).
[37] C. J. Bashor, N. C. Helman, S. Yan, and W. A. Lim, Science **319**, 1539 (2008).